0026-895X/11/8005-911–919$25.00
MOLECULAR PHARMACOLOGY
Copyright © 2011 The American Society for Pharmacology and Experimental Therapeutics
Mol Pharmacol 80:911–919, 2011

Vol. 80, No. 5
73726/3724021
Printed in U.S.A.

The Pharmacological Profile of Brain Liver Intestine Na^+ Channel: Inhibition by Diarylamidines and Activation by Fenamates

Dominik Wiemuth and Stefan Gründer

Department of Physiology, Rheinisch-Westfälische Technische Hochschule Aachen University, Aachen, Germany

Received May 24, 2011; accepted August 9, 2011

ABSTRACT

The brain liver intestine Na^+ channel (BLINaC) is a member of the degenerin/epithelial Na^+ channel gene family of unknown function. Elucidation of the physiological function of BLINaC would benefit greatly from pharmacological tools that specifically affect BLINaC activity. Guided by the close molecular relation of BLINaC to acid-sensing ion channels, we discovered in this study that rat BLINaC (rBLINaC) and mouse BLINaC are inhibited by micromolar concentrations of diarylamidines and nafamostat, similar to acid-sensing ion channels. Inhibition was voltage-dependent, suggesting pore block as the mechanism of inhibition. Furthermore, we identified the fenamate flufenamic acid and related compounds as agonists of rBLINaC. Application of millimolar concentrations of flufenamic acid to rBLINaC induced a robust, Na^+-selective current, which was blocked partially by amiloride. The identification of an artificial agonist of rBLINaC supports the hypothesis that rBLINaC is opened by an unknown physiological ligand. Inhibition by diarylamidines and activation by fenamates define a unique pharmacological profile for BLINaC, which will be useful to unravel the physiological function of this ion channel.

Introduction

Members of the degenerin (DEG)/epithelial Na^+ channel (ENaC) superfamily are amiloride-sensitive Na^+ channels that are activated and regulated by diverse stimuli and mechanisms, such as protons (Waldmann et al., 1997), peptides (Lingueglia et al., 1995; Golubovic et al., 2007; Dürrnagel et al., 2010), or solely via their surface expression level (Abriel et al., 1999). They are involved in a variety of physiological processes, including Na^+ homeostasis (Canessa et al., 1993), mechanotransduction (O'Hagan et al., 2005), acid-evoked nociception (Jones et al., 2004), and higher brain functions, such as learning and fear conditioning (Wemmie et al., 2002). The block by the diuretic amiloride is a common feature of the DEG/ENaC ion channels, as well as their structure with two transmembrane domains forming a Na^+-selective pore, a large extracellular domain (ECD), and short N and C termini (Canessa et al., 1994; Jasti et al., 2007).

Of the eight DEG/ENaC genes present in the rodent genome, three code for subunits of the constitutively active ENaC ($\alpha\beta\gamma$ENaC) (Canessa et al., 1994) and four code for acid-sensing ion channels (ASIC1–4) (Waldmann et al., 1997; Kellenberger and Schild, 2002). One gene codes for the brain liver intestine Na^+ channel (BLINaC) (Sakai et al., 1999). The function of this channel is completely unknown. The predominant expression of BLINaC in non-neuronal tissues, such as liver, intestine, kidney, and lung, suggests a possible role in epithelial transport. In a previous study, we showed that rat BLINaC (rBLINaC) is inactive, whereas mouse BLINaC (mBLINaC) is constitutively active when expressed in *Xenopus laevis* oocytes (Wiemuth and Gründer, 2010). rBLINaC is blocked by physiological concentrations of extracellular Ca^{2+}, whereas mBLINaC has a drastically decreased Ca^{2+} affinity, which renders mBLINaC constitutively open. In addition, mBLINaC is more selective for Na^+ and has a higher amiloride affinity than rBLINaC. These profound species differences were surprising, because rBLINaC and mBLINaC share 97% of their amino acid sequences. We identified a single amino acid that accounts for the species differences (Wiemuth and Gründer, 2010). These findings suggest that mBLINaC is a constitutively open ENaC,

This work was supported by the START program of the Faculty of Medicine, Rheinisch-Westfälische Technische Hochschule Aachen.
Article, publication date, and citation information can be found at http://molpharm.aspetjournals.org.
doi:10.1124/mol.111.073726.

ABBREVIATIONS: DEG, degenerin; ENaC, epithelial Na^+ channel; ECD, extracellular domain; ASIC, acid-sensing ion channel; BLINaC, brain liver intestine Na^+ channel; rBLINaC, rat brain liver intestine Na^+ channel; mBLINaC, mouse brain liver intestine Na^+ channel; DAPI, 4,6-diamidino-2-phenylindole; HSB, hydroxystilbamidine; FFA, flufenamic acid; NFA, niflumic acid; NMDG, *N*-methyl-D-glucamine; NAFA, nafamostat; DIMI, diminazene; PEN, pentamidine.

whereas rBLINaC is opened by an unknown ligand (Wiemuth and Gründer, 2010).

Despite these recent findings for BLINaC, its physiological function remains unclear. This is partly due to a lack of pharmacological tools that specifically affect the channel. A BLINaC-specific blocker is currently unknown. Diarylamidines, a class of compounds with an antiprotozoal effect, were identified recently as potent blockers of ASICs (Chen et al., 2010b). Because BLINaC is related closely to ASICs (Golubovic et al., 2007), we tested if the diarylamidines pentamidine, 4,6-diamidino-2-phenylindole (DAPI), diminazene, hydroxystilbamidine (HSB), and the related substance nafamostat, another blocker of ASIC activity (Ugawa et al., 2007), affect BLINaC as well. When applied in low micromolar concentrations, all of the tested diarylamidines and nafamostat reversibly inhibited BLINaC currents.

Removal of extracellular Ca^{2+} opens rBLINaC. However, in *X. laevis* oocytes, Ca^{2+} removal also induces a large conductance that may be carried by hemi-gap-junctional channels (Zhang et al., 1998), by Ca^{2+}-inactivated Cl^- channels (Weber et al., 1995a; Weber et al., 1995b), or by both. When using low concentrations of extracellular Ca^{2+} with *X. laevis* oocytes, we routinely inhibit this endogenous conductance by flufenamic acid (FFA) or niflumic acid (NFA). While performing these experiments, we found that FFA not only inhibited the endogenous conductance but also strongly activated rBLINaC, whereas mBLINaC was not affected.

Taken together, we identified in this study diarylamidines as potent inhibitors of rBLINaC and mBLINaC and fenamates, FFA in particular, as agonists of rBLINaC. These compounds provide a new set of pharmacological tools, useful to unravel the physiological function of BLINaC.

Materials and Methods

Molecular Biology. Cloning of rBLINaC (GenBank accession no. NM_022227) and mBLINaC (GenBank accession no. NM_0021370) and generation of complementary RNA were described previously (Wiemuth and Gründer, 2010).

Electrophysiology. Electrophysiological studies in *X. laevis* oocytes using the two-electrode voltage clamp technique were performed as reported previously (Wiemuth and Gründer, 2010). In brief, stage V or VI oocytes of *X. laevis* were injected with 0.08 to 0.16 ng of mBLINaC RNA, 0.3 to 8 ng of rBLINaC RNA, or 0.16 ng of $\alpha\beta\gamma$ENaC, respectively, and kept in low Na^+ OR-2 medium [5 mM NaCl, 77.5 mM *N*-methyl-D-glucamine (NMDG), 2.5 mM KCl, 1.0 mM Na_2HPO_4, 5.0 mM HEPES, 1.0 mM $MgCl_2$, 1.0 mM $CaCl_2$, and 0.5 g/l polyvinylpyrrolidone] at 19°C for 24 to 48 h after injection. Whole-cell currents were recorded at room temperature with a Turbo TEC-03X amplifier using an automated, pump-driven solution exchange system (NPI Electronic GmbH, Tamm, Germany), allowing a fast (300 ms) exchange of the bath solution (Chen et al., 2006). Data acquisition and solution exchange were managed using CellWorks, version 5.1.1 (NPI Electronic GmbH). Data were filtered at 20 Hz and acquired at 1 kHz. Holding potential was −70 mV if not stated otherwise. The bath solution for two-electrode voltage clamp contained 140 mM NaCl, 1.8 mM $CaCl_2$, 1.0 mM $MgCl_2$, and 10 mM HEPES. Low Ca^{2+} bath solutions contained 140 mM NaCl, 10 mM HEPES, 2 mM EDTA, and adequate amounts of $CaCl_2$.

Data Analysis. Data were collected and pooled from at least two preparations of oocytes isolated on different days from different animals, if not stated otherwise. Data were analyzed with IgorPro (Wavemetrics, Lake Oswego, OR) and are presented as means ± S.E.M. Statistical significance was calculated using Student's unpaired *t* test.

At a holding potential of −70 mV, the apparent inhibitory constants (K_i) for the different inhibitors were calculated using the equation $I = I_0/(1 + ([B]/K_i)^{n_H})$, where [B] is the concentration of the blocker, I is the remaining current in the presence of the blocker, I_0 is the current in the complete absence of the blocker, and n_H is the Hill coefficient.

Because for mBLINaC the Hill coefficient n_H for diminazene, nafamostat, and amiloride at a holding potential of −70 mV was close to 1 (n_H ranging from 0.98 to 1.13), we fixed n_H to 1 and estimated K_i at different holding potentials with the following simplification of the previous equation: $K_i = [B](I/I_0 - I)$. The voltage dependence of the block was then analyzed using the Woodhull (1973) model for channel block: $K_i(V) = K_i(0)\exp(z'FV/RT)$, where $K_i(0)$ is the apparent inhibitory constant at 0 mV, z' is the product of the valence of the blocking ion and the fraction of the transmembrane electric field (δ) acting on the ion, V is the membrane potential, F is the Faraday constant, R is the gas constant, and T is absolute temperature.

Chemicals. FFA, NFA, diclofenac, pentamidine, DAPI, diminazene, HSB, and amiloride were purchased from Sigma-Aldrich Laborchemikalien (Seelze, Germany). Structures presented in Figs. 1 and 4 were drawn using CS ChemDraw Ultra (CambridgeSoft Corporation, Cambridge, MA) based on structures available from PubChem (http://pubchem.ncbi.nlm.nih.gov/).

Results

Diarylamidines Are Potent Inhibitors of BLINaC Activity. As reported previously (Wiemuth and Gründer, 2010), expression of mBLINaC in *X. laevis* oocytes resulted in robust currents with an amplitude of several microamperes. Application of 100 μM nafamostat and the diarylamidines pentamidine, DAPI, diminazene, and HSB inhibited the current, with the following rank order diminazene = nafamostat > DAPI > HSB > pentamidine (Fig. 1A; $n = 10$). The weak constitutive current of rBLINaC also was inhibited by nafamostat and the diarylamidines (see below).

We determined the concentration dependence for the two most potent inhibitors, diminazene and nafamostat (Fig. 1, C and D); Fig. 1B shows the chemical structures of amiloride, diminazene, and nafamostat. Increasing concentrations of diminazene and nafamostat were applied to oocytes expressing rBLINaC or mBLINaC. The amplitude of BLINaC currents was estimated by replacing Na^+ with $NMDG^+$, and the current inhibited by diminazene or nafamostat was then normalized to the amplitude of the current decrease in the presence of NMDG, representing the current carried by Na^+. The BLINaC current was blocked almost completely by 100 μM diminazene or 200 μM nafamostat, respectively (Fig. 1, C and D). The inhibitory constants (K_i), calculated using the equation $I = I_0/(1 + ([B]/K_i)^{n_H})$, were not significantly different between rBLINaC and mBLINaC and between diminazene and nafamostat (Fig. 1, C and D). For rBLINaC, K_i was 3.5 ± 0.6 μM ($n = 12$) for diminazene and 5.5 ± 1 μM ($n = 12$) for nafamostat. For mBLINaC, K_i was 2.1 ± 0.3 μM ($n = 12$) for diminazene and 3.8 ± 0.5 μM ($n = 12$) for nafamostat. This is in contrast to observations made for amiloride, although mBLINaC is inhibited by low micromolar concentrations of amiloride, and inhibition of rBLINaC requires millimolar concentrations (Wiemuth and Gründer, 2010). Hill coefficients for diminazene and nafamostat were larger for mBLINaC than those for rBLINaC (1.13 ± 0.04 versus 0.54 ± 0.09 and 0.98 ± 0.06 versus 0.54 ± 0.06; $n = 10$; $p < 0.01$).

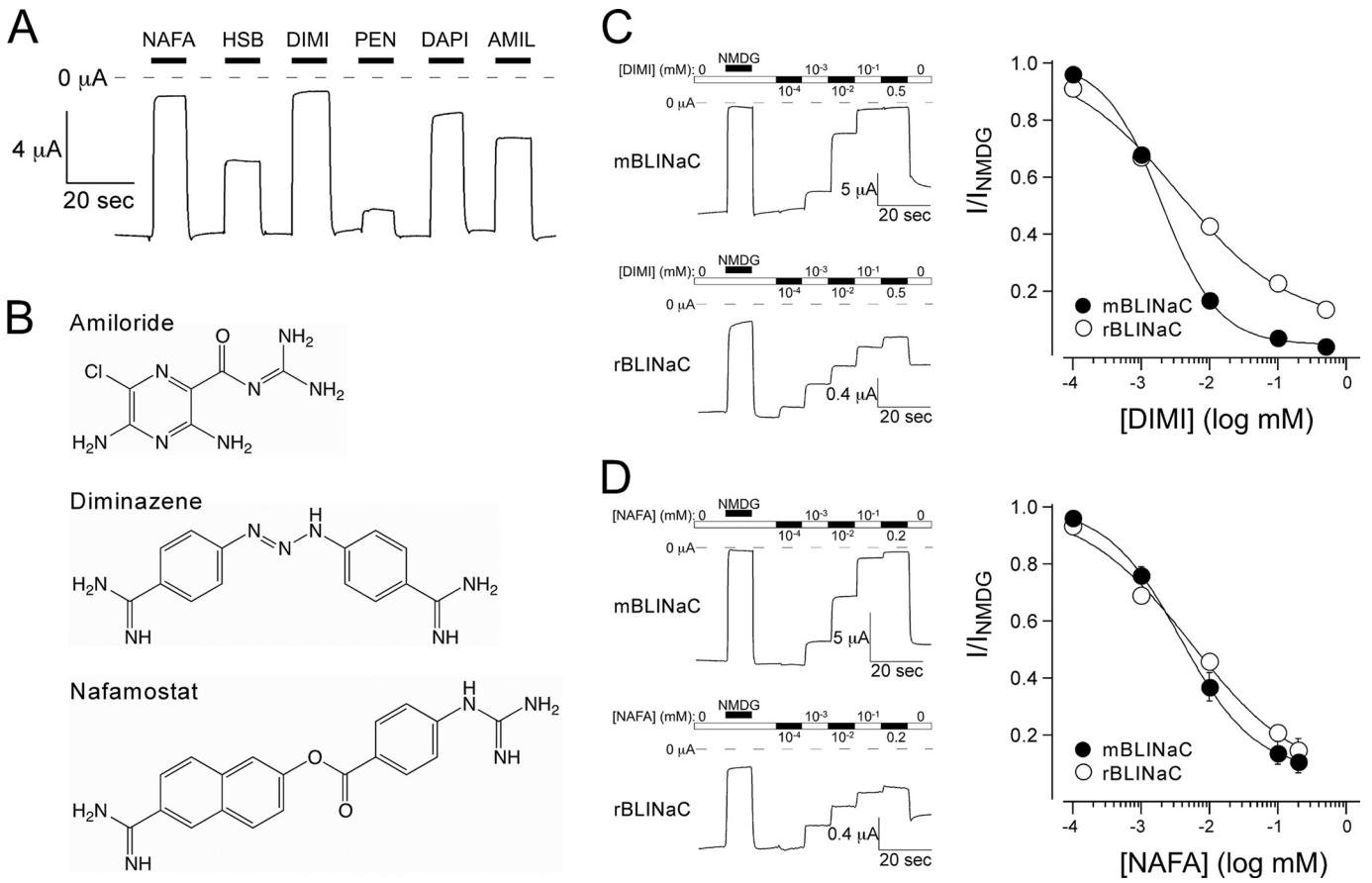

Fig. 1. Nafamostat and diarylamidines reversibly inhibit BLINaC. A, representative current trace of an oocyte expressing mBLINaC. Nafamostat (NAFA), HSB, diminazene (DIMI), pentamidine (PEN), and DAPI were applied at a concentration of 100 μM, and amiloride was applied at a concentration of 10 μM. B, chemical structures of the BLINaC inhibitors amiloride, diminazene, and nafamostat in their uncharged forms. C, concentration-dependent inhibition of rBLINaC and mBLINaC by diminazene. Left, representative current traces; right, concentration-response curves. D, concentration-dependent inhibition of rBLINaC and mBLINaC by nafamostat. Left, representative current traces; right, concentration-response curves. Currents were normalized to the total current carried by Na^+. Holding potential was −70 mV. Error bars represent S.E.M., and curves were fitted to the Hill equation [$I = I_0/(1 + ([B]/K_i)^{nH})$; $n = 10$].

The Block of BLINaC by Diminazene and Nafamostat Is Voltage Dependent. The block of DEG/ENaC channels by the diuretic amiloride is voltage dependent (Palmer, 1984), with stronger block at more negative membrane potentials. The voltage dependence of amiloride arises from its monovalent cationic nature and its binding site within the ion pore. Diminazene and nafamostat are divalent cations carrying two amidine groups. We therefore addressed whether the block of BLINaC by diminazene and nafamostat is also voltage dependent and determined the current-voltage relations of mBLINaC in the absence and the presence of the blockers (100 μM). In the absence of the inhibitors, mBLINaC had a linear current-voltage relation with a reversal potential of +12 ± 0.5 mV ($n = 15$). In the presence of the inhibitors, however, the current-voltage relation was slightly outwardly rectifying. At negative membrane potentials, all three blockers strongly inhibited mBLINaC currents. At positive membrane potentials, however, the efficiency of the block declined, this effect being more pronounced for diminazene and nafamostat than that for amiloride (Fig. 2A). The blockers did not affect the reversal potential. On the basis of the relative block, we estimated the apparent inhibitory constants K_i of diminazene, nafamostat, and amiloride at different membrane potentials according to the equation $K_i = [B](I/I_0 - I)$. This analysis revealed voltage dependence for all three blockers. K_i varied from values in the low micromolar range at negative holding potentials to up to 30-fold higher values at positive holding potentials (Fig. 2B). Assuming that the voltage dependence arises from binding of the blocker within the pore of the channel, one can calculate the fraction of the electric field sensed by the blocking ion according to the Woodhull (1973) model. By fitting the data to the equation $K_i(V) = K_i(0)\exp(z'FV/RT)$, we estimated the fraction of the transmembrane electric field sensed by diminazene and nafamostat to be ~25% ($\delta = 0.26 \pm 0.04$ and 0.27 ± 0.03, respectively; $n = 15$). The estimated fraction of the transmembrane field sensed by amiloride was slightly but significantly larger ($\delta = 0.35 \pm 0.02$; $n = 15$; $p < 0.05$), suggesting that diminazene and nafamostat do not bind as deeply within the pore as amiloride.

Competition of Diminazene and Amiloride for the Same Binding Site in the Pore Region. It is well accepted that amiloride blocks ENaC by binding within the pore. By homology, the same mechanism is assumed to account for block of ASICs and BLINaC by amiloride. Using a computational approach, however, Chen et al. (2010b) predicted that diarylamidines bind to a site at the outer surface of the ECD of ASIC1a. In fact, voltage dependence of the block also can arise from the electric field acting on the channel to alter the affinity or availability of the binding site of the blocker (Hille,

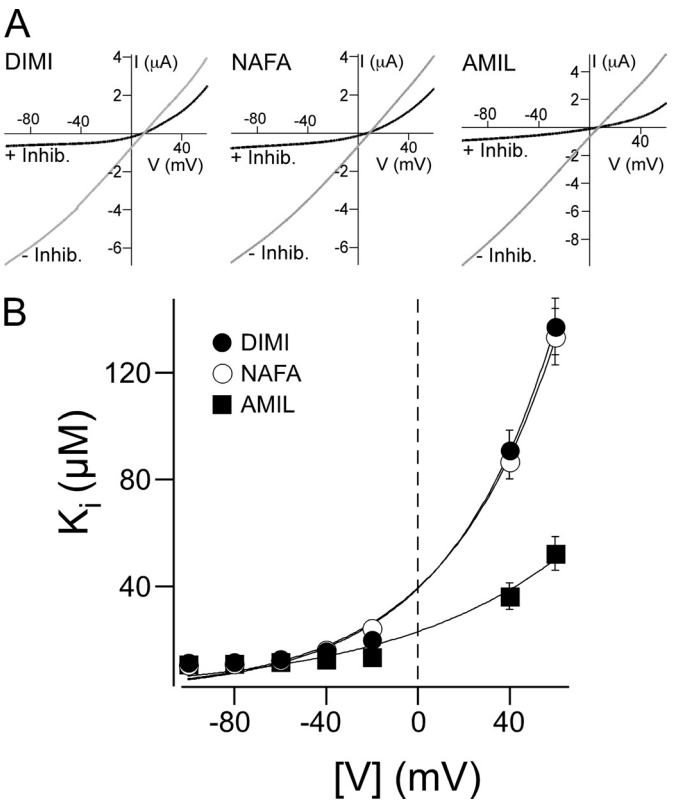

Fig. 2. The inhibition of BLINaC by diarylamidines is voltage dependent. A, averaged current-voltage relationships (n = 10) of mBLINaC in the absence (gray curves) and presence (black curves) of a 100 μM concentration of the inhibitors diminazene, nafamostat, and amiloride. Holding potential was increased continuously from −100 to +60 mV in 9 s. B, the apparent inhibition constant K_i for diminazene (black circles), nafamostat (open circles), and amiloride (black squares) is plotted against the holding potential. K_i values were estimated according to the equation K_i = [B]($I/I_0 - I$). Fit of the data to the equation $K_i(V) = K_i(0)\exp(z'FV/RT)$ is represented by the solid lines and gave δ values of 0.26 ± 0.02, 0.27 ± 0.02, and 0.35 ± 0.01 (n = 15) for diminazene, nafamostat, and amiloride, respectively.

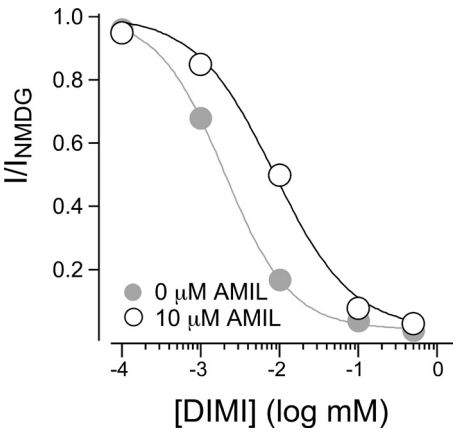

Fig. 3. Apparent affinity of mBLINaC for diminazene is shifted in the presence of amiloride. Concentration-dependent inhibition of mBLINaC by diminazene in the presence (open circles) of 10 μM amiloride. The dose-response curve for diminazene in the absence of amiloride (gray circles) from Fig. 1B is shown for comparison. IC_{50} values were 2.1 ± 0.2 μM (n = 12) in the absence of amiloride and 9.7 ± 0.9 μM (n = 12) in the presence of 10 μM amiloride. Currents were normalized to the total current carried by Na^+. Lines represent a fit to the Hill equation. Holding potential was −70 mV. Error bars represent S.E.M.

2001). Therefore, to find additional evidence that diminazene and nafamostat indeed function as pore blockers, we tested whether amiloride and diminazene compete for the same binding site on BLINaC and determined the concentration-dependent inhibition of diminazene for mBLINaC in the presence of 10 μM amiloride (Fig. 3). Compared with the inhibition of diminazene in the absence of amiloride (K_i = 2.1 ± 0.2 μM; n = 12), the concentration-response curve for diminazene in the presence of 10 μM amiloride was shifted significantly to the right as shown in Fig. 3 ($K_{i,10amil}$ = 9.7 ± 0.9 μM; n = 12; $p < 0.05$). The inhibitory constant K_i of diminazene in the absence ($K_{i,dimi}$) and the presence of amiloride ($K_{i,app}$) can be related by the equation $K_{i,app} = K_{i,dimi}(1 + [amil]/K_{i,amil})$. Using $K_{i,dimi}$ = 2.1 μM, $K_{i,amil}$ = 2.7 μM (n = 12, data not shown), and [amil] = 10 μM, a theoretical value $K_{i,app}$ = 9.9 μM can be calculated that is virtually identical to the value determined experimentally. Thus, our results suggest that diminazene and amiloride compete for an overlapping site in the pore of mBLINaC.

Rat BLINaC Is Strongly Activated by FFA and Related Drugs. Fenamates such as FFA and NFA are known modulators of a wide spectrum of ion channels (White and Aylwin, 1990; McCarty et al., 1993; Ottolia and Toro, 1994; Wang et al., 1997; Lee and Wang, 1999; Peretz et al., 2005; Fernandez et al., 2008; Dai et al., 2010). We routinely use 100 μM FFA or NFA to block the large endogenous conductance that is induced in *X. laevis* oocytes by the removal of extracellular Ca^{2+} (Wiemuth and Gründer, 2010). Using FFA on BLINaC-expressing oocytes, we noticed that it has an activating effect on rBLINaC. As described in previous studies (Sakai et al., 1999; Wiemuth and Gründer, 2010), rBLINaC expressed in *X. laevis* oocytes generated currents only slightly above the background currents observed in uninjected oocytes. These currents were in the range of 0.5 to 1.1 μA and blocked only by high concentrations of amiloride (4 mM). The extracellular application of 1 mM FFA, NFA, or diclofenac to uninjected oocytes did not alter the magnitude of the background current (data not shown). However, application of 1 mM FFA to oocytes expressing rBLINaC induced a large peak inward current (19.6 ± 1.7 μA; n = 12) that rapidly decreased to a lower steady-state level (79.7 ± 1.7% of peak current; n = 12). The application of 1 mM NFA or diclofenac also increased the current amplitude but to a lesser extent (1.7 ± 0.2 and 3.5 ± 0.4 μA, respectively; n = 12); a peak current was not observed (Fig. 4A). The onset of the current increase was very rapid, and the activation of rBLINaC by all three compounds tested was reversible. In contrast to FFA and NFA, diclofenac induced a biphasic current: a fast current increase was followed by a slow increase. FFA, NFA, and diclofenac increased current amplitudes by factors of 20, 4, and 2, respectively (Fig. 4B). Because of its low solubility in water, FFA was predissolved in ethanol and subsequently dissolved in standard bath solution; diclofenac and NFA were dissolved in dimethyl sulfoxide. rBLINaC current amplitude, however, was not affected by the vehicle alone (1% ethanol or dimethyl sulfoxide; data not shown), however, suggesting that the activation of rBLINaC was elicited specifically by the drugs.

Although mBLINaC is 97% identical to rBLINaC, the channel is constitutively open because of its low affinity for extracellular Ca^{2+}, has a high affinity for amiloride (K_i = 2.7 ± 0.3 μM), and furthermore is selective for Na^+ over K^+ (Wiemuth and Gründer, 2010). We tested whether mBLINaC

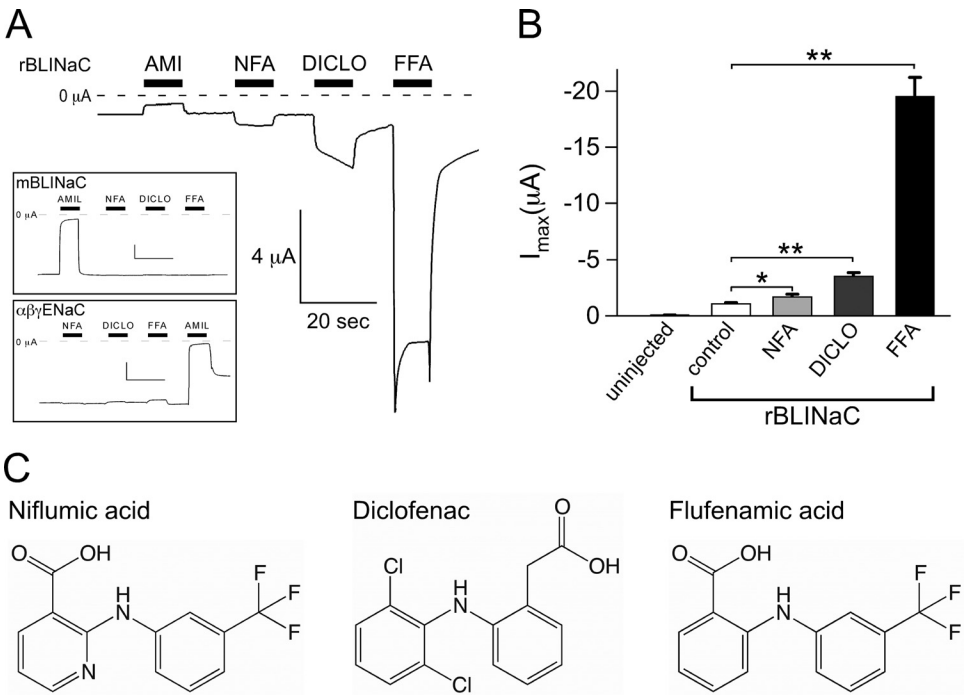

Fig. 4. Fenamates activate rBLINaC. A, representative current traces from oocytes expressing rBLINaC, mBLINaC (top inset), or αβγENaC (bottom inset). Application of 1 mM FFA, NFA, and diclofenac rapidly and reversibly induced inward currents in rBLINaC-expressing oocytes but not in mBLINaC-expressing oocytes. FFA generated the highest rBLINaC current amplitude. αβγENaC showed weak inhibition upon application of FFA. rBLINaC currents were blocked partly by 4 mM amiloride, and mBLINaC currents were reduced strongly by the application of 100 μM amiloride. rBLINaC complementary RNA was injected undiluted, and mBLINaC and αβγENaC complementary RNA were injected 50-fold diluted; currents were recorded in 1.8 mM extracellular Ca^{2+}; holding potential was −70 mV. B, Comparison of maximal current amplitudes of rBLINaC-expressing oocytes induced by the application of FFA, NFA, or diclofenac, respectively (1 mM each; $n = 12$; *, $p < 0.05$; **, $p < 0.005$). C, chemical structures of the BLINaC activators FFA, NFA, and diclofenac in their uncharged forms.

also reacts differently to fenamates than rBLINaC. None of the three compounds that affected rBLINaC had any effect on the current amplitude of mBLINaC (Fig. 4A). We also tested whether αβγENaC is affected by fenamates. Although NFA and diclofenac had no effect, FFA weakly inhibited the activity of the channel (Fig. 4A).

FFA Increases the BLINaC Response to Ca^{2+} Removal. rBLINaC is inhibited almost completely by physiological concentrations of extracellular Ca^{2+}, with an IC_{50} value of ~10 μM (Wiemuth and Gründer, 2010); removal of Ca^{2+} activates the channel. We next addressed the question whether extracellular Ca^{2+} also inhibits the FFA-induced rBLINaC current. In oocytes injected with a 1:25 dilution of rBLINaC complementary RNA, decreasing the concentration of extracellular Ca^{2+} from 1.8 mM to 10 nM strongly increased the current amplitude 8.4-fold from 0.5 ± 0.1 to 4.2 ± 0.4 μA (Fig. 5, A and B; $n = 8$), similar to what we observed previously (Wiemuth and Gründer, 2010). The application of 1 mM FFA at 1.8 mM extracellular Ca^{2+} increased the current amplitude to 4.6 ± 0.4 μA. When applied at 10 nM extracellular Ca^{2+}, 1 mM FFA increased the current further to 34.5 ± 4.9 μA. Hence, in the presence of FFA, decreasing the Ca^{2+} concentration from 1.8 mM to 10 nM increased the current 7.5-fold, very similar to the increase in the absence of FFA. Thus, 1.8 mM Ca^{2+} inhibited the current to the same extent in the absence and presence of FFA. Moreover, because 10 nM Ca^{2+} no longer inhibits rBLINaC (Wiemuth and Gründer, 2010), these results show that FFA activates rBLINaC in a Ca^{2+}-independent manner, ruling out, for example, chelation of Ca^{2+} as the mechanism by which FFA activates rBLINaC.

Dose Dependence of BLINaC Activation by FFA. FFA potentiated rBLINaC activity more strongly than NFA and diclofenac. As a result of low solubility of NFA and diclofenac, we only determined the concentration dependence of the FFA-induced current (Fig. 6A). FFA was only soluble up to 2 mM in our standard bath solution, precluding a precise determination of the EC_{50} value. Fit of the data to the Hill equation yielded an estimate of the apparent EC_{50} value of 2.4 ± 0.7 mM (Fig. 6B). Furthermore, we determined the concentration dependence of the FFA-induced current in the presence of 10 nM extracellular Ca^{2+}. In our standard bath solution containing 10 nM Ca^{2+}, FFA was only soluble up to 1 mM. Fit of the data to the Hill equation yielded an estimate of the apparent EC_{50} value of 1.5 ± 0.9 mM (Fig. 6B), which was not significantly different from the value with 1.8 mM Ca^{2+} ($p < 0.6$). Thus, as with other ion channels, FFA affects rBLINaC in millimolar concentrations. Furthermore, our

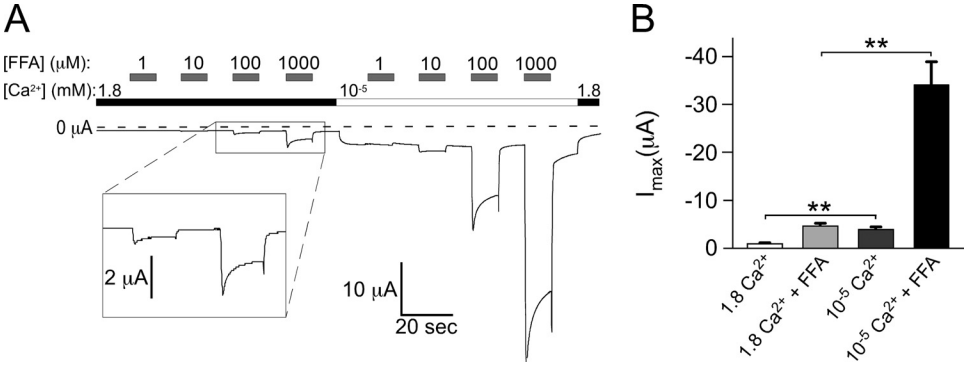

Fig. 5. Ca^{2+} removal increases the FFA-induced BLINaC current. A, representative current trace of rBLINaC in 1.8 mM and 10 nM extracellular Ca^{2+} and different concentrations of FFA. B, comparison of the maximal current amplitudes of rBLINaC-expressing oocytes induced by decreasing the extracellular Ca^{2+} concentration to 10 nM and by applying 1 mM FFA ($n = 8$; **, $p < 0.005$) alone or in combination.

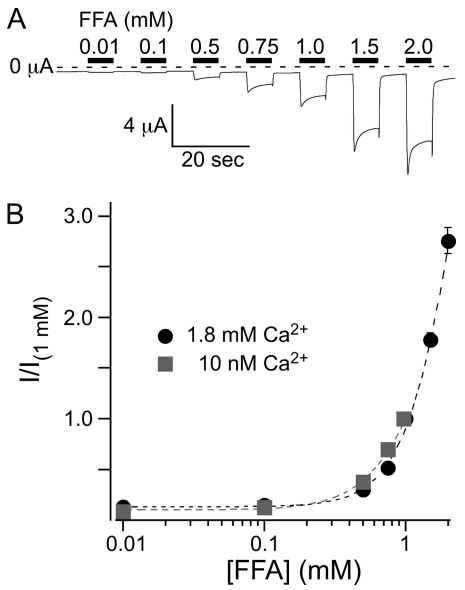

Fig. 6. Dose dependence of the activation of rBLINaC by FFA. A, representative current trace of rBLINaC activated repetitively by the application of increasing concentrations of FFA. B, concentration-response curves for FFA in 1.8 mM extracellular Ca^{2+} (circles) and 10 nM extracellular Ca^{2+} (squares). Error bars represent S.E.M., and dotted lines represent fits to the Hill equation. Peak current amplitudes were normalized to the peak amplitude obtained for 1 mM FFA ($n = 8$). Maximum solubility of FFA was reached at 2 mM in a standard bath solution containing 1.8 mM Ca^{2+} and at 1 mM in a standard bath solution containing 10 nM Ca^{2+} and 2 mM EDTA.

data suggest that the affinity for FFA is independent of the extracellular Ca^{2+} concentration.

When FFA (1 mM) was applied to rBLINaC in normal extracellular Ca^{2+}, coapplication of 100 μM diminazene and nafamostat (Fig. 7A) strongly reduced the FFA-induced current; the inhibition was reversible. The FFA-induced current also was reduced by 1 mM amiloride but to a lesser extent. The apparent inhibitory constant K_i of rBLINaC for diminazene in the presence of FFA was 4.2 ± 0.4 μM ($n = 10$) (Fig. 7B), similar to the K_i in the absence of FFA and to the K_i of constitutively active mBLINaC (Fig. 1B). Sensitivity of the FFA-induced current to diminazene and nafamostat further confirms that the FFA-induced current originates from rBLINaC.

FFA Increases Na^+ Selectivity of rBLINaC. rBLINaC is characterized by an unselective ion pore, and upon relief of the Ca^{2+} block the channel becomes more selective for Na^+ (Wiemuth and Gründer, 2010). We previously proposed that rBLINaC has at least two states: one state of low activity and an unselective ion pore and one state of high activity and a Na^+-selective ion pore (Wiemuth and Gründer, 2010). Because FFA activated rBLINaC, we investigated whether it also increases the Na^+ selectivity of rBLINaC and determined the reversal potential in the absence and presence of 1 mM FFA. The reversal potential of oocytes expressing rBLINaC in the absence of FFA was −11.5 ± 1.8 mV ($n = 12$), similar to what we reported previously (Wiemuth and Gründer, 2010), indicating an unselective pore. In the presence of FFA, the reversal potential of rBLINaC shifted by 20 mV to the right to +9.6 ± 1.5 mV (Fig. 8A; $n = 12$), indicating that, similar to the removal of extracellular Ca^{2+}, selectivity is altered and the channel becomes more selective for Na^+. Because of the comparatively low affinities of diminazene

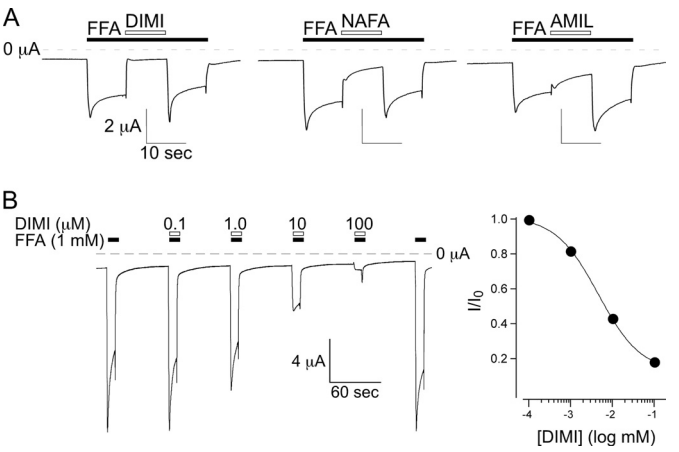

Fig. 7. FFA-induced BLINaC currents are sensitive to diarylamidines and amiloride. A, representative current traces of rBLINaC-expressing oocytes. The current induced by 0.5 mM FFA is inhibited by additional application of 100 μM diminazene or nafamostat. Application of 1 mM amiloride reduced the FFA-induced current only weakly. B, concentration-dependent inhibition of FFA-activated rBLINaC by diminazene. Left, representative current trace; the current induced by 1 mM FFA is inhibited by coapplication of increasing concentrations of diminazene; right, concentration-response curve. Currents were normalized to the maximal current in the absence of diminazene. Holding potential was −70 mV. Error bars represent S.E.M., and the line represents a fit to the Hill equation [$I = I_0/(1 + ([B]/K_i)^{nH})$; $n = 10$].

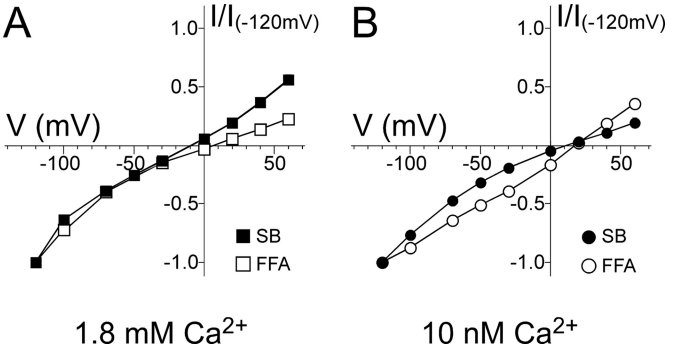

Fig. 8. FFA increases Na^+ selectivity of rBLINaC. A, normalized mean current-voltage relationships ($n = 12$) of peak currents of rBLINaC in 1.8 mM extracellular Ca^{2+} (black squares) and in 1.8 mM Ca^{2+}/1 mM FFA (gray squares). B, normalized mean current-voltage relationships ($n = 12$) of peak currents of rBLINaC in 10 nM extracellular Ca^{2+} (black squares) and in 10 nM Ca^{2+}/1 mM FFA (gray squares). The holding potential was increased stepwise from −120 to +60 mV (20- to 30-mV steps).

and nafamostat at positive membrane potentials and their low solubilities in the presence of FFA, we could not determine the leak current in those measurements. Therefore, we cannot exclude the possibility that the apparent increase in Na^+ selectivity was partly due to a larger ratio of BLINaC to leak conductances.

Finally, we tested whether the selectivity of rBLINaC in low extracellular Ca^{2+} is increased further by FFA. The reversal potential of rBLINaC in 10 nM extracellular Ca^{2+} was +14.7 ± 2.1 mV ($n = 12$), similar to what we reported previously (Wiemuth and Gründer, 2010). Application of FFA shifted the reversal potential slightly but significantly ($p < 0.001$) further to the right to +20.9 ± 2.3 mV (Fig. 8B; $n = 12$), indicating an increased selectivity for Na^+ in the presence of FFA. In summary, in both low (10 nM) and normal (1.8 mM) extracellular Ca^{2+}, FFA increased the Na^+ selectivity of rBLINaC.

Discussion

In this study, we elaborated on the pharmacological profile of rBLINaC and mBLINaC. We identify diarylamidines and nafamostat as potent inhibitors of mBLINaC and rBLINaC and fenamates, in particular FFA, as activators of rBLINaC. These results will help to identify the BLINaC current in native cells and tissues and thereby contribute to a better understanding of the physiological function of BLINaC.

The predominant expression of BLINaC in non-neuronal tissues (Sakai et al., 1999; Schaefer et al., 2000) suggests that it might be involved in epithelial transport, like ENaC (Wiemuth and Gründer, 2010). mBLINaC is characterized by a large constitutive activity and a high Na^+ permeability (Wiemuth and Gründer, 2010), properties that are very similar to ENaC. The apparent inhibitory constant for block by amiloride is also similar, although 5- to 10-fold larger for BLINaC than that for ENaC. The highly similar properties of currents carried by mBLINaC and ENaC make their distinction difficult. In this study, however, we found that BLINaC is highly sensitive to diarylamidines and nafamostat. ENaC, in contrast, is insensitive to these drugs (Chen et al., 2010b), providing an easy means to distinguish between BLINaC and ENaC currents in native tissues.

There are few reports in the literature of Na^+-selective currents that are sensitive to amiloride and that cannot be attributed unequivocally to ENaC expression. Those currents include a Na^+-selective channel from rabbit proximal tubules (Gögelein and Greger, 1986; Jacobsen et al., 1988) that is sensitive to Ca^{2+} (Blokkebak-Poulsen et al., 1991) and a Na^+ channel in LLC-PK1 cells (Raychowdhury et al., 2004), a cell line with proximal tubule characteristics derived from pig kidney. Furthermore, several studies describe an amiloride-insensitive and thus ENaC-independent pathway for Na^+ entry in epithelial cells of various organs, such as lung (Shlyonsky et al., 2005), colon (Inagaki et al., 2004), and esophagus (Awayda et al., 2004). Because its affinity for amiloride is low, rBLINaC might be a candidate responsible for these currents. Future studies will show whether BLINaC underlies some of those conductances in epithelial cells.

In contrast to ENaC, ASICs share inhibition by diarylamidines and nafamostat with BLINaC (Ugawa et al., 2007; Chen et al., 2010b). This common pharmacology of ASICs and BLINaC is in agreement with their close evolutionary relationship on a common branch within the DEG/ENaC gene family (Golubovic et al., 2007); however, ENaC is on a different branch. Peptide-gated Na^+ channels from Hydra, the HyNaCs, are on the same branch as ASICs and BLINaC (Golubovic et al., 2007) and indeed also are sensitive to diarylamidines (S. Dürrnagel and S. Gründer, unpublished observations), further confirming that the common pharmacology might reflect close sequence homology.

We show that inhibition of BLINaC by the diarylamidine diminazene and by nafamostat is voltage-dependent and that diminazene competes with amiloride for binding to the channel. Assuming that amiloride binds within the pore of BLINaC, as is accepted generally for ENaC, these results suggest that diminazene and probably nafamostat also bind within the pore of BLINaC. Our results indicate that they do not bind as deeply in the pore as amiloride, which is explained readily by their larger sizes. However, it is important to mention that a variety of factors, for example, surface charges at the entry of the ion pore, may influence the fraction of the transmembrane electric field apparently acting on the ion. Such factors could render the localization of the binding site solely based on the Woodhull model imprecise.

Although we investigated voltage dependence only for diminazene and nafamostat, given the similar structures of different diarylamidines (Chen et al., 2010a), it is possible that the other diarylamidines (that is, pentamidine, DAPI, and HSB) inhibited BLINaC by binding within the pore, too. The mechanism of ASIC inhibition by diarylamidines is unknown. On the basis of a computational "docking" approach, however, a binding site on the outer surface of the ECD of ASICs was proposed (Chen et al., 2010b). Among other limitations, such a docking approach may be limited by the fact that the crystal structure of chicken ASIC1, which was used in this approach, represents the desensitized conformation, whereas diarylamidines apparently inhibit open ASICs (Chen et al., 2010b). Assuming that the closely related BLINaC shares its mechanism of inhibition with ASICs, it should be considered that the binding site of diarylamidines on ASICs is not on the ECD but within the ion pore.

In contrast to mBLINaC, which is constitutively active, rBLINaC is blocked tightly by physiological concentrations of extracellular Ca^{2+} (Wiemuth and Gründer, 2010). This led us to speculate that rBLINaC is activated by an unknown ligand. Moreover, we proposed a two-state model for rBLINaC with one state of low activity that has Ca^{2+} tightly bound and an unselective ion pore and a second state of high activity that has no Ca^{2+} bound and a Na^+-selective ion pore (Wiemuth and Gründer, 2010). The putative ligand would shift the equilibrium distribution between these two states (Wiemuth and Gründer, 2010). Our discovery that FFA activates rBLINaC is in agreement with the idea that FFA shifts the equilibrium distribution toward the state of high activity. Moreover, FFA increases the Na^+ selectivity of the pore as expected if the high-activity state becomes more populated. For mBLINaC, the majority of channels are already in the high-activity state, explaining why FFA was ineffective for mBLINaC. Thus, FFA behaves like an artificial ligand for rBLINaC. The discovery of an artificial ligand for rBLINaC confirms our two-state model and renders the existence of a natural ligand that activates rBLINaC even more likely. This natural ligand may have structural similarities to FFA. Because of the insolubility of FFA at higher concentrations, we could not determine the apparent affinity of FFA precisely. But it was of rather low affinity, being in the low millimolar range. The putative natural ligand probably will have a significantly higher affinity.

Fenamates affect various other ion channels. On the one hand, they inhibit cystic fibrosis transmembrane conductance regulator (McCarty et al., 1993), Ca^{2+}-activated Cl^- channels of *X. laevis* oocytes (White and Aylwin, 1990), kidney ClC-K Cl^- channels (Liantonio et al., 2006), and the voltage-gated K^+ channel Kv2.1 (Lee and Wang, 1999). On the other hand, they activate large-conductance Ca^{2+}-activated K^+ channels (Ottolia and Toro, 1994) and modify the gating of Kv4.3 (Wang et al., 1997) and KCNQ2/3 (Peretz et al., 2005). Furthermore, they increase the activity of hERG1 (Fernandez et al., 2008) and strongly activate the Na^+-activated K^+ channel Slo2.1 (Dai et al., 2010). In most of these cases, effective concentrations of the fenamates were in the millimolar range, similar to the activation of rBLINaC.

The FFA-induced BLINaC current was time dependent: an initial peak current declined to a smaller steady-state level. Upon washout, the current then briefly increased again before the channels deactivated (Fig. 4). Such behavior is explained most easily by a dual effect of FFA on BLINaC: besides activating the channel, FFA apparently also inhibited the channel. Activation was stronger, probably because activation had a higher affinity than inhibition. Activation at lower concentrations than inhibition also could explain why the low-potency agonists NFA and diclofenac did not induce currents with a similar time dependence as FFA. At higher concentrations, which we could not achieve due to the limited solubility of the drugs, they may well do so. A dual effect of fenamates with activation and inhibition also has been reported previously for ClC-K Cl^- channels (Liantonio et al., 2006; Liantonio et al., 2008).

In a recent study, Macianskiene et al. (2010) discovered that FFA induced an unselective cation current in cardiomyocytes from sheep and pig. The molecular nature of the channel responsible for this current was not unraveled; DEG/ENaC channels were excluded as candidates, because the current was not sensitive to 10 μM amiloride. The ion selectivity and pharmacology of BLINaC from sheep and pig are unknown, but if they have the same properties as rBLINaC, it would be possible that the FFA-induced current observed by Macianskiene et al. (2010) might be carried by BLINaC. This hypothesis is supported by reverse transcription polymerase chain reaction results from Sakai et al. (1999), who observed weak expression of rBLINaC in heart. Further experiments are necessary to address the relation of the FFA-induced current in cardiac myocytes to BLINaC.

In summary, we identify diarylamidines as potent inhibitors of BLINaC and fenamates as activators of rBLINaC. These drugs define a unique pharmacological profile for BLINaC that will allow the identification of BLINaC currents in native cells and tissues, which is an important step toward unraveling the physiological function of this channel.

Acknowledgments

We thank A. Oslender-Bujotzek and S. Lenz for expert technical assistance.

Authorship Contributions

Participated in research design: Wiemuth and Gründer.
Conducted experiments: Wiemuth.
Performed data analysis: Wiemuth and Gründer.
Wrote or contributed to the writing of the manuscript: Wiemuth and Gründer.

References

Abriel H, Loffing J, Rebhun JF, Pratt JH, Schild L, Horisberger JD, Rotin D, and Staub O (1999) Defective regulation of the epithelial Na^+ channel by Nedd4 in Liddle's syndrome. *J Clin Invest* **103:**667–673.
Awayda MS, Bengrine A, Tobey NA, Stockand JD, and Orlando RC (2004) Nonselective cation transport in native esophageal epithelia. *Am J Physiol Cell Physiol* **287:**C395–C402.
Blokkebak-Poulsen J, Sheikh MI, and Jacobsen C (1991) Effects of divalent cations and pH on amiloride-sensitive Na^+ fluxes into luminal membrane vesicles from pars recta of rabbit proximal tubule. *Biochim Biophys Acta* **1068:**125–132.
Canessa CM, Horisberger JD, and Rossier BC (1993) Epithelial sodium channel related to proteins involved in neurodegeneration. *Nature* **361:**467–470.
Canessa CM, Schild L, Buell G, Thorens B, Gautschi I, Horisberger JD, and Rossier BC (1994) Amiloride-sensitive epithelial Na^+ channel is made of three homologous subunits. *Nature* **367:**463–467.
Chen X, Orser BA, and MacDonald JF (2010a) Design and screening of ASIC inhibitors based on aromatic diamidines for combating neurological disorders. *Eur J Pharmacol* **648:**15–23.
Chen X, Paukert M, Kadurin I, Pusch M, and Gründer S (2006) Strong modulation by RFamide neuropeptides of the ASIC1b/3 heteromer in competition with extracellular calcium. *Neuropharmacology* **50:**964–974.
Chen X, Qiu L, Li M, Dürrnagel S, Orser BA, Xiong ZG, and MacDonald JF (2010b) Diarylamidines: high potency inhibitors of acid-sensing ion channels. *Neuropharmacology* **58:**1045–1053.
Dai L, Garg V, and Sanguinetti MC (2010) Activation of Slo2.1 channels by niflumic acid. *J Gen Physiol* **135:**275–295.
Dürrnagel S, Kuhn A, Tsiairis CD, Williamson M, Kalbacher H, Grimmelikhuijzen CJ, Holstein TW, and Gründer S (2010) Three homologous subunits form a high affinity peptide-gated ion channel in Hydra. *J Biol Chem* **285:**11958–11965.
Fernandez D, Sargent J, Sachse FB, and Sanguinetti MC (2008) Structural basis for ether-a-go-go-related gene K^+ channel subtype-dependent activation by niflumic acid. *Mol Pharmacol* **73:**1159–1167.
Gögelein H and Greger R (1986) Na^+ selective channels in the apical membrane of rabbit late proximal tubules (pars recta). *Pflugers Arch* **406:**198–203.
Golubovic A, Kuhn A, Williamson M, Kalbacher H, Holstein TW, Grimmelikhuijzen CJ, and Gründer S (2007) A peptide-gated ion channel from the freshwater polyp Hydra. *J Biol Chem* **282:**35098–35103.
Hille B (2001) Classical mechanisms of block, in *Ion Channels of Excitable Membranes,* 3rd ed., pp 503–537, Sinauer Associates, Sunderland, MA.
Inagaki A, Yamaguchi S, and Ishikawa T (2004) Amiloride-sensitive epithelial Na^+ channel currents in surface cells of rat rectal colon. *Am J Physiol Cell Physiol* **286:**C380–C390.
Jacobsen C, Røigaard-Petersen H, and Sheikh MI (1988) Demonstration of Na^+-selective channels in the luminal-membrane vesicles isolated from pars recta of rabbit proximal tubule. *FEBS Lett* **236:**95–99.
Jasti J, Furukawa H, Gonzales EB, and Gouaux E (2007) Structure of acid-sensing ion channel 1 at 1.9 A resolution and low pH. *Nature* **449:**316–323.
Jones NG, Slater R, Cadiou H, McNaughton P, and McMahon SB (2004) Acid-induced pain and its modulation in humans. *J Neurosci* **24:**10974–10979.
Kellenberger S and Schild L (2002) Epithelial sodium channel/degenerin family of ion channels: a variety of functions for a shared structure. *Physiol Rev* **82:**735–767.
Lee YT and Wang Q (1999) Inhibition of hKv2.1, a major human neuronal voltage-gated K^+ channel, by meclofenamic acid. *Eur J Pharmacol* **378:**349–356.
Liantonio A, Picollo A, Babini E, Carbonara G, Fracchiolla G, Loiodice F, Tortorella V, Pusch M, and Camerino DC (2006) Activation and inhibition of kidney CLC-K chloride channels by fenamates. *Mol Pharmacol* **69:**165–173.
Liantonio A, Picollo A, Carbonara G, Fracchiolla G, Tortorella P, Loiodice F, Laghezza A, Babini E, Zifarelli G, Pusch M, et al. (2008) Molecular switch for CLC-K Cl^- channel block/activation: optimal pharmacophoric requirements towards high-affinity ligands. *Proc Natl Acad Sci USA* **105:**1369–1373.
Lingueglia E, Champigny G, Lazdunski M, and Barbry P (1995) Cloning of the amiloride-sensitive FMRFamide peptide-gated sodium channel. *Nature* **378:**730–733.
Macianskiene R, Gwanyanya A, Sipido KR, Vereecke J, and Mubagwa K (2010) Induction of a novel cation current in cardiac ventricular myocytes by flufenamic acid and related drugs. *Br J Pharmacol* **161:**416–429.
McCarty NA, McDonough S, Cohen BN, Riordan JR, Davidson N, and Lester HA (1993) Voltage-dependent block of the cystic fibrosis transmembrane conductance regulator Cl^- channel by two closely related arylaminobenzoates. *J Gen Physiol* **102:**1–23.
O'Hagan R, Chalfie M, and Goodman MB (2005) The MEC-4 DEG/ENaC channel of Caenorhabditis elegans touch receptor neurons transduces mechanical signals. *Nat Neurosci* **8:**43–50.
Ottolia M and Toro L (1994) Potentiation of large conductance KCa channels by niflumic, flufenamic, and mefenamic acids. *Biophys J* **67:**2272–2279.
Palmer LG (1984) Voltage-dependent block by amiloride and other monovalent cations of apical Na channels in the toad urinary bladder. *J Membr Biol* **80:**153–165.
Peretz A, Degani N, Nachman R, Uziyel Y, Gibor G, Shabat D, and Attali B (2005) Meclofenamic acid and diclofenac, novel templates of KCNQ2/Q3 potassium channel openers, depress cortical neuron activity and exhibit anticonvulsant properties. *Mol Pharmacol* **67:**1053–1066.
Raychowdhury MK, Ibarra C, Damiano A, Jackson GR Jr, Smith PR, McLaughlin M, Prat AG, Ausiello DA, Lader AS, and Cantiello HF (2004) Characterization of Na^+-permeable cation channels in LLC-PK1 renal epithelial cells. *J Biol Chem* **279:**20137–20146.
Sakai H, Lingueglia E, Champigny G, Mattei MG, and Lazdunski M (1999) Cloning and functional expression of a novel degenerin-like Na^+ channel gene in mammals. *J Physiol* **519:**323–333.
Schaefer L, Sakai H, Mattei M, Lazdunski M, and Lingueglia E (2000) Molecular cloning, functional expression and chromosomal localization of an amiloride-sensitive Na^+ channel from human small intestine. *FEBS Lett* **471:**205–210.
Shlyonsky V, Goolaerts A, Van Beneden R, and Sariban-Sohraby S (2005) Differentiation of epithelial Na^+ channel function. An in vitro model. *J Biol Chem* **280:**24181–24187.
Ugawa S, Ishida Y, Ueda T, Inoue K, Nagao M, and Shimada S (2007) Nafamostat mesilate reversibly blocks acid-sensing ion channel currents. *Biochem Biophys Res Commun* **363:**203–208.
Waldmann R, Champigny G, Bassilana F, Heurteaux C, and Lazdunski M (1997) A proton-gated cation channel involved in acid-sensing. *Nature* **386:**173–177.
Wang HS, Dixon JE, and McKinnon D (1997) Unexpected and differential effects of Cl^- channel blockers on the Kv4.3 and Kv4.2 K^+ channels. Implications for the study of the I(to2) current. *Circ Res* **81:**711–718.
Weber WM, Liebold KM, Reifarth FW, and Clauss W (1995a) The Ca^{2+}-induced leak current in Xenopus oocytes is indeed mediated through a Cl^- channel. *J Membr Biol* **148:**263–275.
Weber WM, Liebold KM, Reifarth FW, Uhr U, and Clauss W (1995b) Influence of extracellular Ca^{2+} on endogenous Cl^- channels in Xenopus oocytes. *Pflugers Arch* **429:**820–824.

Wemmie JA, Chen J, Askwith CC, Hruska-Hageman AM, Price MP, Nolan BC, Yoder PG, Lamani E, Hoshi T, Freeman JH Jr, et al. (2002) The acid-activated ion channel ASIC contributes to synaptic plasticity, learning, and memory. *Neuron* **34:**463–477.
White MM and Aylwin M (1990) Niflumic and flufenamic acids are potent reversible blockers of Ca^{2+}-activated Cl^- channels in *Xenopus* oocytes. *Mol Pharmacol* **37:**720–724.
Wiemuth D and Gründer S (2010) A single amino acid tunes Ca^{2+} inhibition of brain liver intestine Na^+ channel (BLINaC). *J Biol Chem* **285:**30404–30410.
Woodhull AM (1973) Ionic blockage of sodium channels in nerve. *J Gen Physiol* **61:**687–708.
Zhang Y, McBride DW Jr, and Hamill OP (1998) The ion selectivity of a membrane conductance inactivated by extracellular calcium in Xenopus oocytes. *J Physiol* **508:**763–776.

Address correspondence to: Stefan Gründer, Department of Physiology, Rheinisch-Westfälische Technische Hochschule Aachen University, Pauwelsstrasse 30, D-52074 Aachen, Germany. E-mail: sgruender@ukaachen.de